Protist, Vol. 161, 177–196, April 2010
http://www.elsevier.de/protis
Published online date 21 December 2009

Protist

ORIGINAL PAPER

Ultrastructure and 18S rDNA Phylogeny of *Apoikia lindahlii* comb. nov. (Chrysophyceae) and its Epibiontic Protists, *Filos agilis* gen. et sp. nov. (Bicosoecida) and *Nanos amicus* gen. et sp. nov. (Bicosoecida)

Eunsoo Kim[a,1,2,3], Naoji Yubuki[b,3], Brian S. Leander[b], and Linda E. Graham[a]

[a]Department of Botany, University of Wisconsin-Madison, 132 Birge Hall, 430 Lincoln Drive, Madison, WI 53706, USA
[b]Canadian Institute for Advanced Research, Program in Integrated Microbial Biodiversity, Departments of Botany and Zoology, University of British Columbia, 6270 University Boulevard, Vancouver, BC, Canada V6T 1Z4

Submitted January 15, 2009; Accepted September 19, 2009
Monitoring Editor: Robert A. Andersen

Three heterotrophic stramenopiles—*Apoikia lindahlii* comb. nov. (Chrysophyceae), *Filos agilis* gen. et sp. nov. (Bicosoecida), and *Nanos amicus* gen. et sp. nov. (Bicosoecida)—were isolated from acidic peat bogs. The biflagellate *A. lindahlii* forms loose irregular colonies from which swimming cells may detach, and produces extensive mucilaginous material containing bacterial cells. Phylogenetic analyses of small subunit rDNA sequences demonstrated that *A. lindahlii* branches within the Chrysophyceae. While *A. lindahlii* is an obligate heterotroph, ultrastructural observations revealed a leukoplast in the perinuclear region. The pico-sized uniflagellates *F. agilis* and *N. amicus* were isolated from separate lakes and within the mucilage of *A. lindahlii*, suggesting their close associations in natural habitats. In SSU rDNA phylogenies, *F. agilis* and *N. amicus* were closely related to the bicosoecids *Adriamonas*, *Siluania*, *Paramonas*, and *Nerada*. While *Filos*, *Nanos*, and *Siluania* are similar in light microscopic features, their SSU rDNA gene sequences differed significantly (>8% differences) and were not monophyletic. Both *F. agilis* and *N. amicus* have a cytostome/cytopharynx particle ingestion apparatus. Bacterial cells and material similar to the mucilage of *A. lindahlii* occurred within the food vacuole of *F. agilis* and *N. amicus*. The nature of association between *A. lindahlii* and its epibiontic bicosoecids is discussed.

Key words: *Apoikia*; Bicosoecida; Chrysophyceae; *Filos*; *Nanos*; stramenopiles.

[1]Corresponding author; fax +1 902 494 1355
e-mail eunsookim@dal.ca (E. Kim).
[2]Present address: Department of Biochemistry and Molecular Biology, Dalhousie University, 5850 College Street, Halifax, NS, Canada B3H 1X5.
[3]Both authors equally contributed to this work.

doi:10.1016/j.protis.2009.09.003

Introduction

Free-living heterotrophic and mixotrophic stramenopiles can play an important role in food web ecology because some consume large numbers of bacteria and/or dissolved organic molecules (Jones 2000). For instance, the recently identified marine stramenopile (MAST) groups represent up to 35% of heterotrophic flagellates (<5 μm) in surface ocean samples, suggesting their great contribution to bacterivory and nutrient re-cycling in such habitats (Massana et al. 2006). Within the stramenopiles, members of several subclades, such as labyrinthulomycetes, opalinids, and bicosoecids, lack plastids and are obligate heterotrophs (Moriya et al. 2000; Sekiguchi et al. 2002). Plastid-containing stramenopiles form a subclade in which the majority of species are phototrophic (Andersen 2004). Loss of photosynthesis has occurred multiple times in this clade, notably in the Chrysophyceae, generating obligate heterotrophs that typically possess remnant plastids (i.e., leukoplasts) in the perinuclear region (Sekiguchi et al. 2002).

Environmental small subunit (SSU) rDNA gene sequencing surveys have demonstrated a high hidden diversity of microbial eukaryotes, including stramenopiles, in various aquatic habitats (e.g. Berney et al. 2004; López-García et al. 2001). A study of bacterial and eukaryotic diversity in a peat bog noted that heterotrophic flagellates of such habitats have been poorly characterized (Graham et al. 2004). Peat bogs, together with minerotrophic fens, comprise peatlands, a biogeochemically-important ecosystem that sequesters about one-third of global soil carbon (Gorham 1991). Peat bogs and fens cover about 2-3% of global landmass, mostly located in the Northern hemisphere, and are characterized by low pH, usually between 4 and 5, due to the acidifying *Sphagnum* mosses (Crum 1992). Here, we report molecular phylogenetic and ultrastructural analyses that describe three heterotrophic stramenopiles isolated from peat bogs in Wisconsin, USA: the colonial, mucilage-producing, leukoplast-containing *Apoikia lindahlii* comb. nov. and its two epibiontic, plastidless picoflagellates—*Filos agilis* gen. et. sp. nov. and *Nanos amicus* gen. et. sp. nov.

Results

General Features of *Apoikia lindahlii* comb. nov.

Two strains of the colonial flagellate, *Apoikia lindahlii* comb. nov. (JYME1 and HOOK2) were isolated from two acidic lakes in Wisconsin. *Apoikia lindahlii* usually formed swimming colonies of cells held together by mucilage (Fig. 1A). The cells typically occurred in a single hemispherical layer (Figs 1A, 2A), but the shapes and the sizes of the colonies were not uniform and sometimes branched colonies formed. The size of a single non-branched colony can be up to about 500 μm in diameter comprising over one hundred cells, although most colonies occurred in smaller sizes (data not shown). The composition of the culture medium seemed to affect colony formation. For example, when the organic nutrient level was low, the total amount of mucilage was reduced and more solitary cells were observed. No cytoplasmic connections were observed among the cells of colonies, and micropipetting easily disrupted colonies, releasing individual cells. Detached cells were able to produce new colonies. The ovoid cells measured 6–8 μm and had one long anterior flagellum (about six times the length of the cell) and a second short flagellum that was not easily seen by light microscopy (Figs 1B, 3A). The flagellate cells actively fed on bacterial cells and other particles that were attached to the mucilage. Colonies moved in a more or less straight line, while solitary cells swam in a spiral pattern.

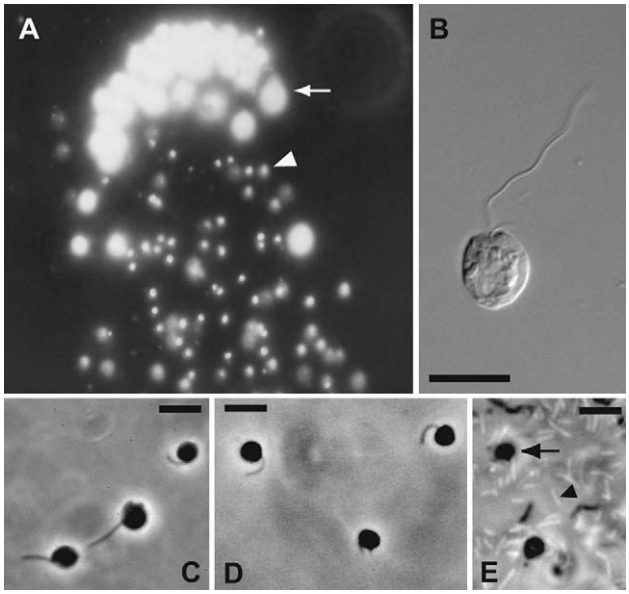

Figure 1. Light micrographs of *Apoikia lindahlii, Filos agilis*, and *Nanos amicus.* – **A**. A colony of *A. lindahlii* (arrow) and its epibiont *F. agilis* (arrowhead). **B**. *Apoikia lindahlii.* **C**. *Nanos amicus.* **D**. *Filos agilis.* **E.** *Filos agilis* (arrow) and bacterial cells (arrowhead) within *A. lindahlii* mucilage. Scale bar=10 μm (B), 5 μm (C, D, E).

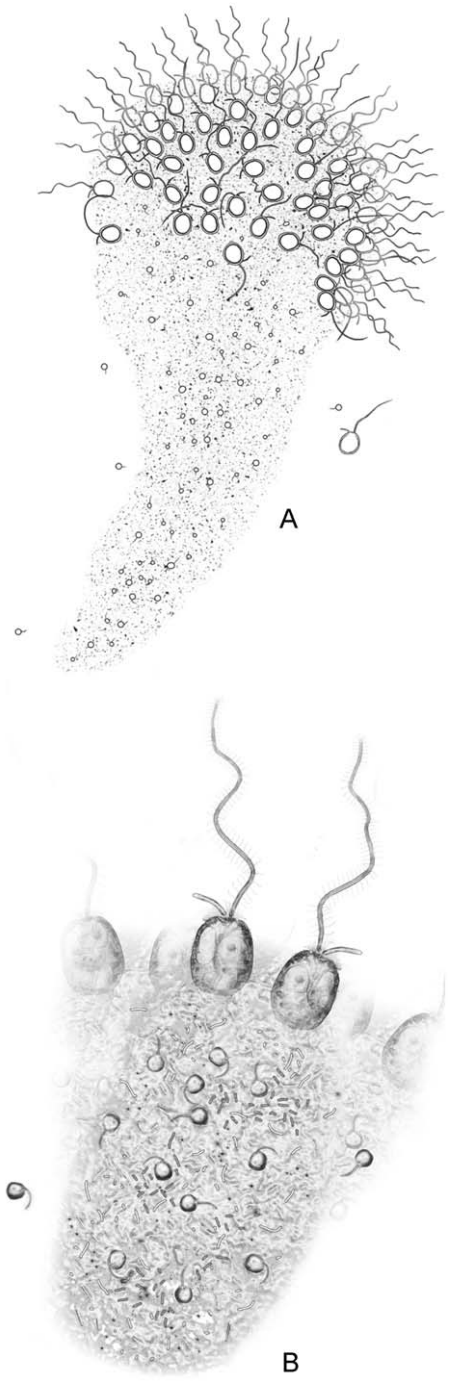

Figure 2. Drawings of *Apoikia lindahlii* and its epibiotic bicosoecids. – **A**. A colony of *A. lindahlii*. **B**. The mucilaginous matrix of *A. lindahlii* and the epibiotic bicosoecids and bacteria.

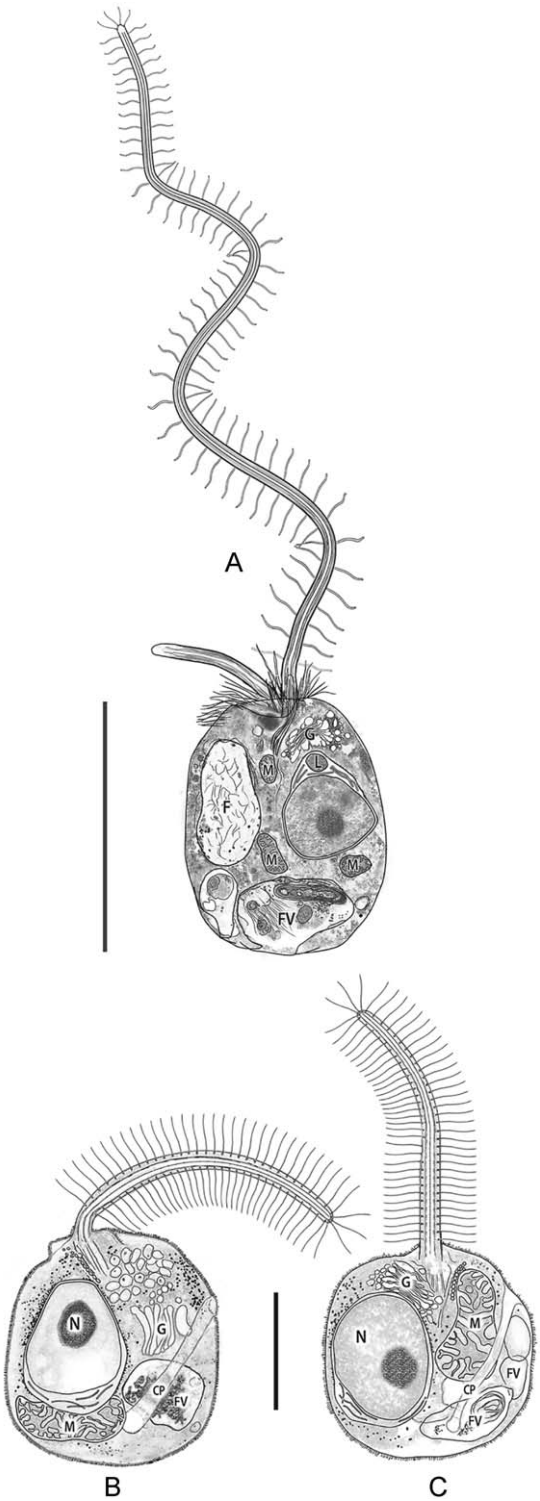

Figure 3. Composite drawings – **A**. *Apoikia lindahlii* **B**. *Nanos amicus* **C**. *Filos agilis*. CP=cytopharynx, F=fibrillo-granular vesicle, FV=food vacuole, G=Golgi body, L=leukoplast, M=mitochondrion, N=nucleus. Scale bar=7 μm (A), 1.5 μm (B, C).

Pigmentation was not observed after *Apoikia* had been exposed to light for periods of 7–20 days, indicating that this organism is an obligate heterotroph. Statospore (siliceous resting cyst) formation was not observed.

Ultrastructural data demonstrated that each cell of *Apoikia* possessed a mastigoneme (flagellar hair)-bearing anterior flagellum (AF), a short posterior flagellum (PF), a nucleus, a single Golgi body located near the anterior end of the cell, and several mitochondria with tubular cristae (Figs 4–7). Food vacuoles that included bacterial prey cells were located near the posterior part of the cell (Fig. 5A). Numerous tubular mastigonemes were attached to the cell surface near the flagella (Fig. 5D, E) and vesicles containing fibrillo-granular contents were observed (Fig. 5D). A network of endoplasmic reticulum (ER) extended from the nucleus to the cell surface (Fig. 5F). Neither a flagellar swelling nor a paraflagellar rod was observed on the PF (Fig. 5D, G). The cells also lacked scales (Figs 4A, 5A, B). The perinuclear region contained tubular mastigonemes (Fig. 5E, G, I) and a vestigial chloroplast (i.e. a leukoplast) that was bounded by four membranes (Figs 5D, G, H, 7A).

Basal Bodies and the Rootlet Complex of *Apoikia lindahlii* comb. nov.

All of the interphase cells examined in this study had two mature basal bodies and one auxiliary immature barren basal body (Figs 5D, 6G). The anterior basal body (AB) and the posterior basal body (PB) anchored the anterior flagellum (AF) and the posterior flagellum (PF), respectively, and were arranged at a ~85 degree angle to each other. The transitional zones between the basal bodies and axonemes contained a transitional helix with 4-5 gyres, a transitional plate, an axosome, and transitional fibers (Fig. 5C, D). The AB and the PB were linked by three connecting fibers (Fig. 6H). The immature barren basal body (BB) was located at the left side of the PB (Fig. 6G, H). The BB possessed neither the transitional fibers nor the anchoring flagellum, but did contain the flagellar transitional plate and the axosome. All three basal bodies contained cart-wheel structures and were 670 nm in length. A rhizoplast consisted of two types of striated fibers: a thick fiber and a thin fiber (Fig. 5E). The thick fiber was 130 nm thick with a 120 nm periodicity and originated from the posterior side of the PB. The thin fiber was 33 nm in thick with a 110 nm periodicity and extended from the dorsal side of the AB. The rhizoplast was at least 2 μm long, extended toward the posterior end of the cell, and ran between the nucleus and a conspicuous Golgi body. A basal aggregate was observed near the posterior side of the AB and PB (Fig. 6G).

The overall arrangement of the flagellar apparatus of *A. lindahlii* was consistent with and clearly homologous to the flagellar apparatus in other well-studied Chrysophyceae. Therefore, we applied the terminology used in Moestrup (2000) to describe *A. lindahlii*. The numbering scheme used to characterize the root system is based on the process of flagellar transformation. Accordingly, root 1 (R1), root 2 (R2), root 3 (R3), and root 4 (R4) in Moestrup's terminology are equivalent to R4, R3, R1, and R2 in the scheme used in Andersen (1987, 1989) (Fig. 8).

The PB was linked to two microtubular roots: root 1 (R1) and root 2 (R2). These two roots formed the rim of the cellular depression within which the PF resided (Fig. 7A–E). R1 consisted of three microtubules and originated from the anterior left side of the PB (Fig. 7A, F, G). At its origin, R1 possessed a lamellar structure on the side facing the PB, and this lamella connected R1 to the PB. R1 ran beneath the cell surface to the left of the cell and extend clockwise, forming a loop (Fig. 6B–F).

R2 consisted of 6-7 microtubules that collectively formed a trough-like structure (Fig. 6A–F). R2 originated from the connecting fiber, which linked the AB to the PB on the right side of the cell. Two microtubules from R2 extended further than the others and split into two directions; these two microtubules extended counter-clockwise when viewed from the anterior end of the cell and followed the path of the R1 microtubules, but in the opposite direction. Together, microtubules from R1 and R2 joined together at the left side of the PB and formed a prominent curvature (Fig. 6A–F). The two microtubules of R2 returned to the posterior side of PB. Bacteria (and other small food particles) were captured between them (Fig. 6K–M).

The AB was linked to two microtubular roots: root 3 (R3) and root 4 (R4) (Fig. 6I, J). R3 consisted of three microtubules that extended from the dorsal side of the AB to the left side of the cell (Fig. 6A–F). R3 was associated with a dense lamella, which formed the microtubule-organizing center (MTOC). The cytoplasmic microtubules arose from the dense lamella and supported the dorsal side of the cell in a rib-like fashion. R3 and the right-hand cytoplasmic microtubules were

linked to a fibrous structure positioned near the origin of R3 (Fig. 6I). A single microtubule formed R4 and originated from the ventral side of the AB on the right side of the cell. This microtubule extended between R1 and R3 on the left side of the cell (Fig. 6J).

LM and TEM Observations of *Filos agilis* and *Nanos amicus*

Filos agilis gen. et sp. nov. and *Nanos amicus* gen. et sp. nov. were co-isolated with the *A. lindahlii* strain HOOK1 and strain JYME2, respectively. Both flagellates were primarily embedded in the mucilage of *A. lindahlii*, though some occurred outside the mucilage (Figs 1A, 2A, B). *Filos agilis* and *Nanos amicus* were similar in morphology. Both were extremely tiny, measuring about 2–3 μm, with a single thick flagellum about as long as the cells (Fig. 1C, D). These picoflagellates grew abundantly within the mucilage of *A. lindahlii* and did not appear to be eaten by it. When free in the water, both picoflagellates swam in a straight line, and the flagellum moved very quickly. The cells sometimes tumbled around violently when escaping from the mucilage or under the pressure of a cover slip. These picoflagellates could be grown separately from *A. lindahlii*, but were more abundant in association with *A. lindahlii*.

Ultrastructural studies demonstrated that *F. agilis* and *N. amicus* both possess a cytostome/cytopharynx apparatus (Figs 9B, F, 10A). A large food vacuole linked to the cytopharynx contained bacterial cells or amorphous material (Fig. 9A, E). Cell surfaces were covered with an organic layer, except near the point of the flagellar insertion (Figs 9G, 10C). The surface of the single flagellum was covered with mastigonemes (Figs 9A, 10B). Structures similar to tubular mastigonemes occurred in the perinuclear region (data not shown). Each cell contained a single nucleus, a single mitochondrion with tubular cristae, and a Golgi body (Figs 9, 10). While we did not detect a second flagellum, 1 or 2 additional basal bodies were sometimes observed (Fig. 9C). In *F. agilis*, a rootlet consisting of 8 microtubules, in a 7+1 arrangement, occurred near the basal bodies (Fig. 9C), and a similar rootlet composed of at least 7 microtubules occurred deeper in the cytoplasm (not shown). A broad rootlet composed of 6 microtubules (Fig. 10D), which occurred as 4 or 4+1 microtubules deeper in the cell of *N. amicus*, was observed. In addition, both picoflagellates possessed two additional rootlets consisting of 1

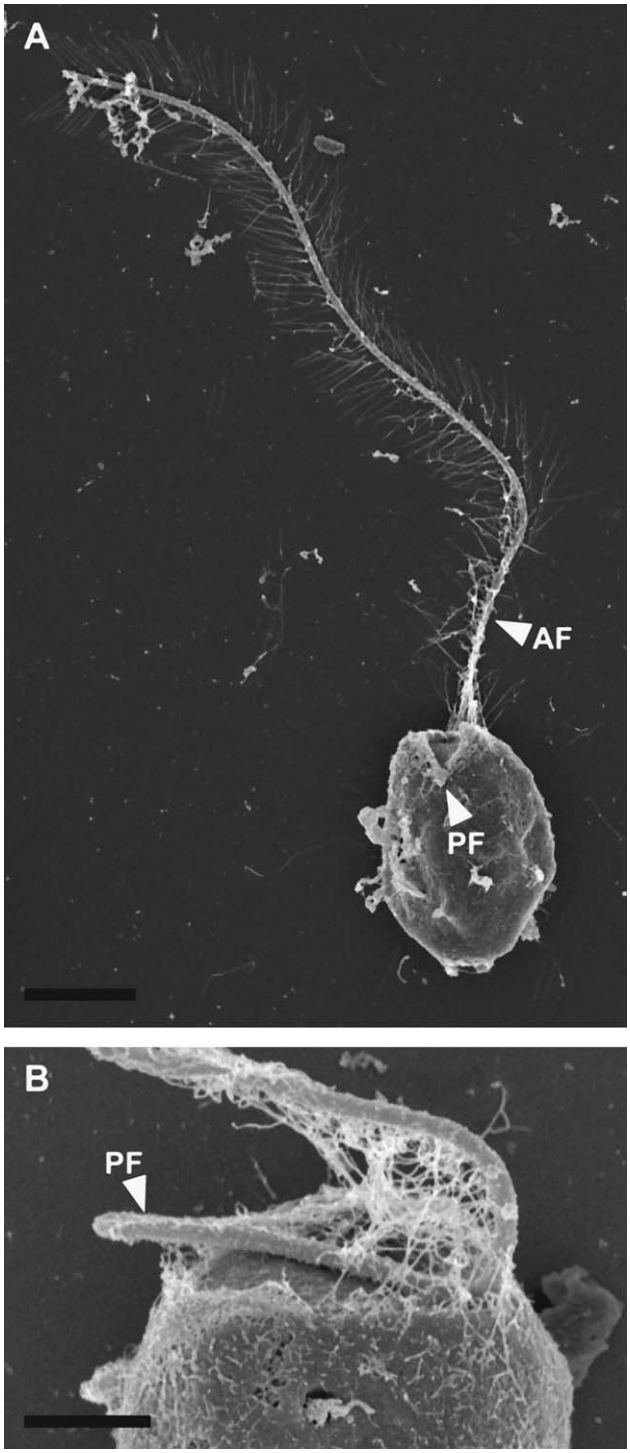

Figure 4. Scanning electron micrographs of *Apoikia lindahlii*. **A** Image showing the anterior flagellum (AF) bearing mastigonemes and the posterior flagellum (PF). Note that scales were not present on the cell surface. Scale bar=2.5 μm. **B** High magnification view of the cell showing the short PF lying within a cell depression. Scale bar=1 μm.

and 2 microtubules, although these may split from the broad rootlet.

Filos agilis and *Nanos amicus* differed in some structural and behavioral features. For example, *N. amicus* was slightly larger in cell length (2.8 μm, n=10) than *F. agilis* (2.5 μm, n=10). The mitochondrion in *F. agilis* was located close to the basal body, but that of *N. agilis* occurred in a posterior position (Fig. 3B, C). *Filos agilis* moved at least twice as fast as *N. agilis*. When swimming, *F. agilis* moved straight for

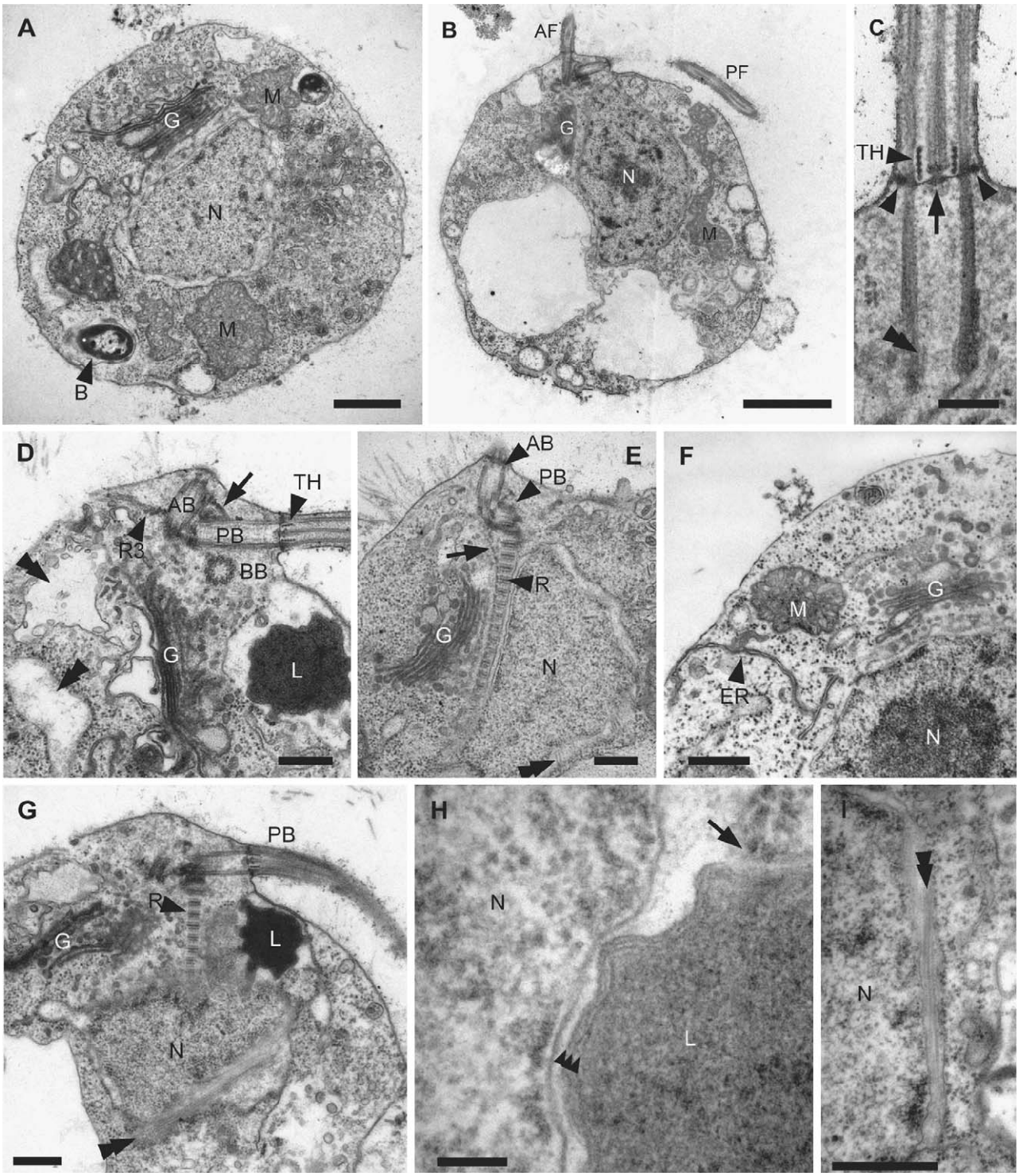

about 50–100 μm before changing direction. In contrast, *N. amicus* moved straight for about 10–20 μm before changing direction. Populations of *N. amicus* usually grew more densely in *A. lindahlii* mucilage than did those of *F. agilis*.

Phylogenetic Analyses of SSU rDNA Sequences

Molecular phylogenetic analyses of SSU rDNA sequences demonstrated that *A. lindahlii*, *F. agilis*, and *N. amicus* are stramenopiles (Fig. 11). *Apoikia lindahlii* branched within the well-supported Chrysophyceae+Synurophyceae clade. A subsequent analysis narrowly focusing on this clade, which included more positions and more taxa, suggested that *A. lindahlii* is closely related to two uncultured chrysophytes and the *Spumella*-like JMB08 strain (100% ML bootstrap value), which is likewise heterotrophic, but not colonial (Fig. 12). However, ultrastructural analysis has not yet been accomplished for the JMB08 strain (Boenigk et al. 2005). While relationships among major subclades of Chrysophyceae+Synurophyceae were poorly resolved, *A. lindahlii* branched within clade E as defined by Andersen et al. (1999) (Fig. 12).

Phylogenetic analyses of SSU rDNA sequences indicated that *F. agilis* and *N. amicus* are bicosoecids. A clade including these two flagellates, *Nerada*, *Paramonas*, *Siluania*, and *Adriamonas*, was supported with moderate to strong bootstrap values (Fig. 11). When environmental bicosoecid sequences were included in the analysis, three morphospecies *F. agilis*, *N. amicus*, and *Siluania monomastiga* did not form a clade (Fig. 13). The branching order of major subclades of bicosoecids was not well supported. The mean differences among SSU rDNA sequences of three morphospecies ranged between 8.54% and 11.68% (Table 1).

Discussion

Phylogeny and Classification of *Apoikia lindahlii* comb. nov.

Müller (1773) originally classified the tiny colorless heterokont flagellate (< 5 μm) within the genus *Monas*. However, due to the small size and relatively simple organization of the cell, the original descriptions, largely based on light microscopic features, did not provide accurate and sufficient information for reliable classification. As a result, the subsequent taxonomic treatments of *Monas* have been very confusing (Boenigk 2008; Preisig et al. 1991; Silva 1960). More recent systematists have subsequently applied *Spumella* or "*Spumella*-like flagellate" instead of *Monas* for tiny colorless heterokont flagellates. This approach has led to additional taxonomic confusion, because *Spumella* is now known to be polyphyletic (Boenigk 2008; Stoeck et al. 2008;

Figure 5. Transmission electron micrographs showing the general ultrastructure of *Apoikia lindahlii*. **A** An oblique section of the cell showing the nucleus (N), the Golgi body (G), mitochondoria with tubular cristae (M) and an ingested bacterium (B). Scale bar=1 μm. **B** A sagittal section of the cell showing the insertion of the anterior and posterior flagella (AF and PF) near the anterior part of the cell. The Golgi body (G) was located near the dorsal side of the nucleus (N). Scale bar=500 nm. **C** The AF and the anterior basal body (AB) contained a transitional helix (TH) with 4-5 gyres, transitional fibers (arrowheads), an axosome (arrow), and a cartwheel structure (double arrowhead). Scale bar=200 nm. **D** Section showing the insertion of the PF near the apex of the cell. The PF possessed a transitional helix (TH) with 4-5 gyres and connecting fibers (arrow). A putative leukoplast (L) was located beneath the PF. Root 3 (R3) possessed cytoplasmic microtubules that were associated with the dorsal side of the AB. The vesicles containing fibrillo-granular contents (double arrowheads) were observed on the dorsal side of the cell. BB=immature barren basal body. Scale bar=500 nm. **E** Section showing the thin fiber of rhizoplast (arrow) originating from the dorsal side of the AB. The thick fiber (R) extended from the posterior side of the posterior basal body (PB). The double arrowhead points to the mastigonemes in the perinuclear region. Scale bar=500 nm. **F** High magnification view of the cell showing the endoplasmic reticulum (ER) extending to the cell surface. Scale bar=500 nm. **G** Longitudinal section through the leukoplast (L) located beneath the PF and the rhizoplast (R). Note the outer nuclear membrane is continuous with the outer membrane of the leukoplast. Mastigonemes can be seen within the perinuclear region (double arrowhead). Scale bar=500 nm. **H** High magnification view showing the leukoplast bounded by three membranes (small arrowheads) and a fourth outer membrane (arrow) that is continuous with the outer nuclear membrane. Scale bar=100 nm. **I** High magnification view of the mastigonemes (double arrowhead) in the perinuclear region. Scale bar=100 nm.

Fig. 12). The small subunit ribosomal gene sequence and ultrastructural data reported in this study further demonstrates the polyphyly of *Spumella* and more comprehensively characterizes the phylogenetic position of our flagellate. A colonial, mucilage-producing colorless stramenopile flagellate forming a single hemispherical layer was reported as *Monas lindahlii* by Skuja (1956). Although the cell size of our isolate was on the small end of the range of cell sizes originally reported for *M. lindahlii* (7-12 μm long, Skuja 1956), we consider *M. lindahlii* to be the closest described species to our isolate. However, in order to avoid further taxonomic confusion by

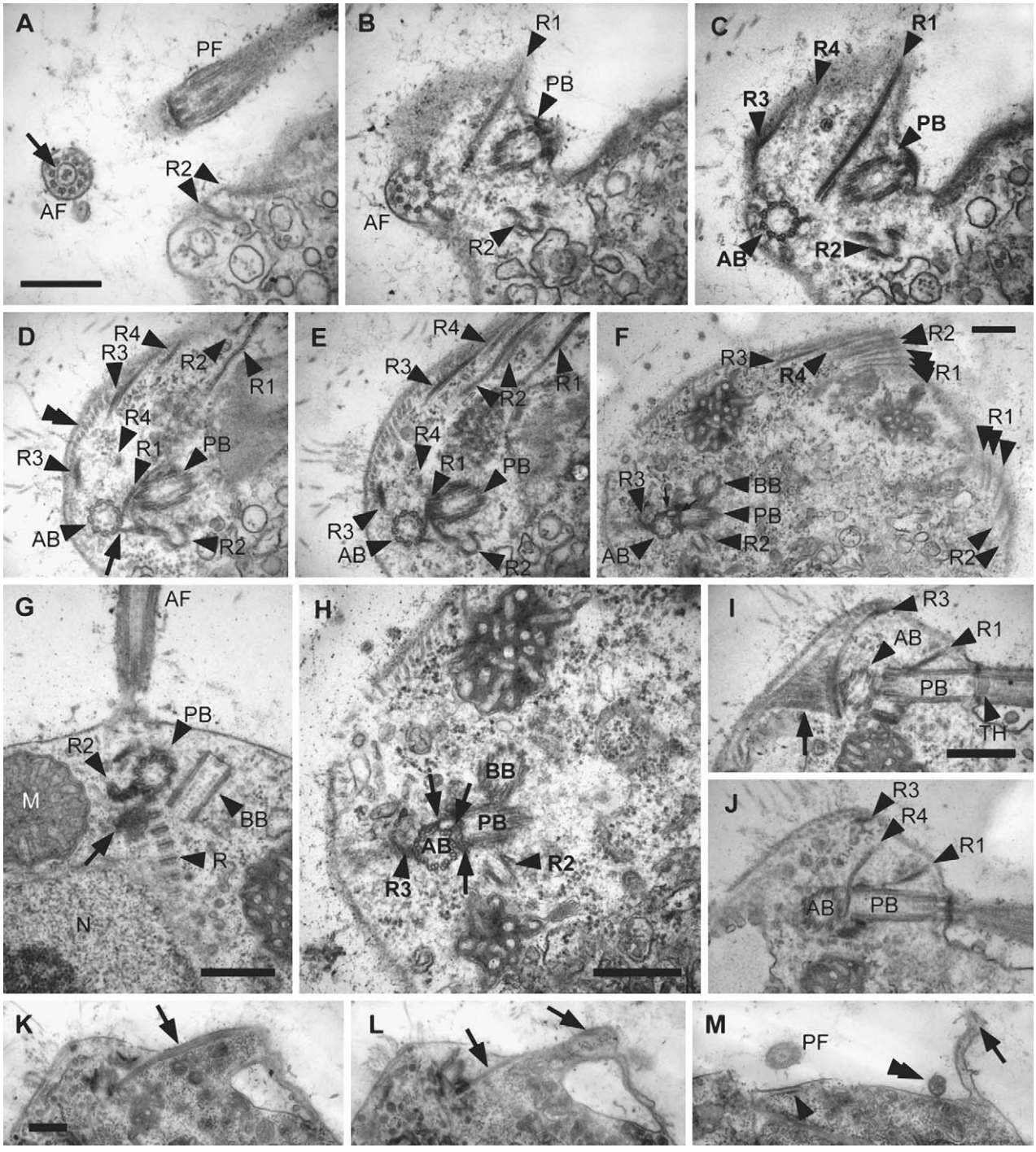

lumping this flagellate into either *Monas* or *Spumella*, we have established the novel genus "*Apoikia*" and have identified our isolate as *Apoikia lindahlii*.

Ultrastructural and SSU rDNA sequence data confirmed that *A. lindahlii* comb. nov. is a heterotrophic stramenopile with two unequal flagella, mastigonemes produced in the perinuclear region, and mitochondria with tubular cristae. This flagellate also possesses synapomorphic features of Chrysophyceae: a transitional helix with 4-5 gyres, a rhizoplast associated with the basal bodies and nucleus (Andersen 1987, 1989; Hibberd 1979). In addition, the following features of the flagellar apparatus are sufficient to assign the organism to the Chrysophyceae: (1) R1 and R2 turn clockwise and counter clockwise, respectively, when viewed from the anterior end of the cell, and both roots support the rim of the cell depression; (2) R2 splits into two directions and forms the feeding basket; and (3) the cytoplasmic microtubules nucleate from R3 and support the dorsal side of the cell.

In photosynthetic Chrysophyceae, the chloroplast is located beneath the anterior depression and associated posterior flagellum (PF), and a stigma is positioned within the apical part of the chloroplast, facing toward the flagellar swelling on the PF. *Apoikia lindahlii* does not have a stigma or the paraflagellar swelling on the PF, but a leukoplast is located under the cellular depression.

Additional similarities between *A. lindahlii* and other Chrysophyceae include (1) the basal aggregation, which has been observed in *Poterioochromonas malhamensis* (Schnepf et al. 1977) and (2) an R1 that curves and terminates much like that in *Uroglena* and *Dinobryon* (Andersen 1990). Moreover, R2 in both *A. lindahlii* and mixotrophic chrysophyceans such as *Epipyxis pulchra* is involved in food capture (Fig. 6M) (Andersen and Wetherbee 1992; Wetherbee and Andersen 1991). In both taxa, two of the six microtubules of R2 contribute to the formation of the feeding basket.

The fibrillo-granular contents of large vesicles are similar to the mucilage that normally surrounds *A. lindahlii* cells. Similar vesicles occur in cells of the mucilage-producing, colonial chrysophycean *Chrysosphaerella brevispina* (Preisig and Hibberd 1983). Several tiny osmophilic globules located at the periphery of the cell were similar to structures in other chrysophyceans that have been interpreted as extrusive organelles (Preisig and Hibberd 1983).

Apoikia lindahlii did not produce pigmentation when grown in the light for as long as 20 days, suggesting that *A. lindahlii* is an obligate heterotrophic flagellate. The greatest similarity is with *Monas lindahliii* and our organism is distinct from several other genera of colonial heterotrophic chrysophyceans, such as *Anthophysa Cladonema*, *Dendromonas*, *Siderodendron*, *Siphomonas*. *Anthophysa* differs from *A. lindahlii* in having a shorter anterior flagellum and a longer posterior flagellum, a more pointed posterior end, and more tightly aggregated colonies. *Anthophysa* can be distinguished from *A. lindahlii* by the paraflagellar swelling on the short flagellum (Belcher and Swale 1972). Individual cells of

Figure 6. The orientation of the four microtubular rootlets (R1, R2, R3 and R4) in *Apoikia lindahlii* (**A-E** at same scale, bar=500 nm; **I-J** at same scale, bar=500 nm). **A-E** Serial sections taken from anterior to posterior. **A** The anterior most section, just before the insertion of two flagella. A cross section of the anterior flagellum (AF) showed the transitional helix (arrow). **B** Section showing the transitional zone of the AF and anterior basal body (AB). R1 extended to the left side of the cell. **C** Section showing the transitional zone of the AF and AB. Four microtubular rootlets (R1-R4) were observed. **D** Section showing the cytoplasmic microtubules originating from R3 (double arrowhead) and supporting the dorsal side of the cell. A connecting fiber (arrow) linked the AB, the PB and R2. **E** Section at the origin of R1 on the anterior side of the PB. Four rootlets ran parallel to each other at the left side of the cell. **F** Section showing the third barren basal body (BB), the turning of R1 and R2, and the origin of R3. Two connecting fibers (small arrows) were located between AB and PB. Scale bar=500 nm. **G** Cell viewed from the ventral side showing the AF, the PB, and immature BB. The rhizoplast (R), root 2 (R2), and basal aggregate (arrow) were associated with the PB. Scale bar=500 nm. **H** Cross section of the apical area of the cell showing three connecting fibers (arrows) that linked the AB with the posterior basal body (PB). The cytoplasmic microtubules nucleated from the dense lamella on R3. Scale bar=500 nm. **I** Section showing the origin of R3. The right most cytoplasmic microtubule linked R3 with a fibrous structure (arrow). **J** Section showing R4 inserted from the gap between the AB and PB. **K-M** Semi-consecutive serial sections showing the R2 is separated into two components that (arrow and arrowhead) support the feeding apparatus and facilitate the capture of bacteria (double arrowhead). Scale bar=500 nm.

Cladonema and *Dendromonas* have triangular cell bodies borne at the tips of a dichotomously branched stalk (Kristiansen and Preisig 2001), thereby differing from *A. lindahlii*. *Siderodendron* produces a more narrow and rigid stalk, which often becomes brown as the result of mineralization (Pringsheim 1946). In contrast, the mucilage of *A. lindahlii* does not become colored. Unlike *A. lindahlii*, the cells of *Siphomonas* are usually embedded singly at the tips of a regularly branched stalk (Pringsheim 1946). In other example, *Spumella* sp. produces a gelatinous sphere within which flagellates swim, but the cells do not form a single layer of colonial flagellates as is observed in *A. lindahlii* (Yubuki et al. 2008).

Certain colony-forming photoautotrophic/mixotrophic Chrysophyceae superficially resemble *A. lindahlii*, but can be distinguished from this species. *Eusphaerella* forms single-layered hemispherical colonies similar to those of *A. lindahlii*, but the colonies are more tightly aggregated, and dense mucilage was not observed (Kristiansen and Preisig 2001). Unlike *A. lindahlii*, the cell body of

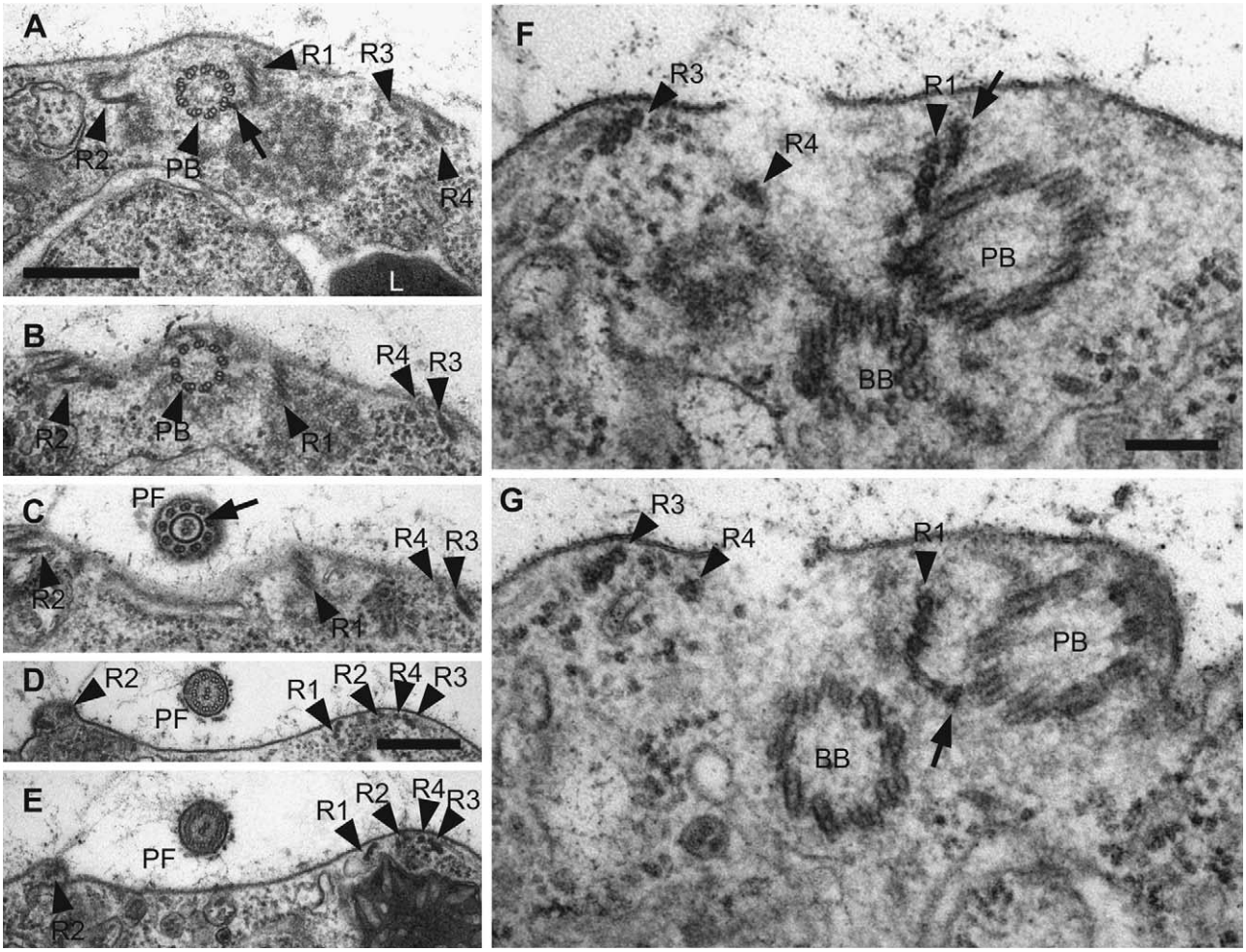

Figure 7. The orientation of the microtubular rootlets of *Apoikia lindahlii* (**A-C** at same scale, bar=500 nm; **D-E** at same scale, bar=500 nm; **F-G** at same scale, bar=200 nm). **A-E** Serial sections of the cell viewed from the tip of the posterior flagellum (PF). **A** Micrograph showing the middle area of the posterior basal body (PB). The lamella structure (arrow) connected R1 to the PB. **B** Image showing the transitional zone of the PF. **C** Image showing the transitional helix (arrow) of the PF. **D** Image showing the rim of the cellular depression that is supported by all four microtubular roots. **E** Image showing R1-R4 and the cytoplasmic microtubule from R3. **F-G** High-magnification serial sections showing R1 and R3. **F** Three microtubules of R1 originate from the anterior side of PF. The root was associated with the lamella structure (arrow). **G** The section showing the lamella structure that is linked to the PB (arrow).

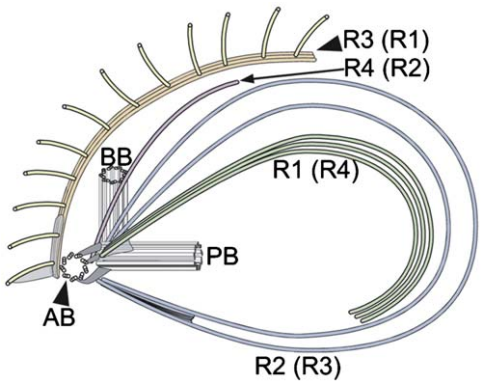

Figure 8. An illustration of the absolute configuration of the flagellar apparatus of *Apoikia lindahlii* as viewed from anterior side of the cell. The numbering system follows the terminology of Moestrup (2000). The parenthetic numberings follow the terminology of Andersen (1987, 1989).

Lepidochrysis is covered with scales (Ikävalko et al. 1994). *Mycochrysis* forms more or less hemispherical colonies anchored to a dense branching column of dense mucilage through a thin gelatinous stalk (Kristiansen and Preisig 2001), which is absent in *A. lindahlii*. *Atraktochrysis* produces mucilage and forms a loose colony similar to that of *A. lindahlii*, but its posterior flagellum is longer than that of *A. lindahlii*. While the colonial habitat of these heterotrophic or photoautotrophic/mixotrophic chrysophyceans suggests that some of these might be closely related to *A. lindahlii*, their SSU rDNA gene sequences are not currently available to test this hypothesis.

Phylogenetic analyses of SSU rDNA sequences demonstrated that *A. lindahlii* branches within clade E in the Chrysophyceae (Fig. 12); this result indicates that *A. lindahlii* has lost photosynthesis secondarily as have several other members of this clade. Heterotrophic chrysophyceans such as *Paraphysomonas* and *Anthophysa* typically possess a leukoplast in the perinuclear region (Belcher and Swale 1972; Preisig and Hibberd 1983). Plastids of the Chrysophyceae are bounded by four surrounding membranes (Preisig and Hibberd 1984) including the plastid ER, which is continuous with the outer nuclear membrane (Gibbs 1979; Preisig and Hibberd 1983). The spherical structure observed in the perinuclear region of *A. lindahlii* (Fig. 5H) is surrounded by four membranes, hence is most likely a leukoplast. In addition to leukoplast, some chrysophyceans possess endosymbiotic bacteria in the perinuclear region (Preisig and Hibberd 1984; Wujek 1984). However, such bacteria can be distinguished from leukoplast by having three membranes (including the nuclear membrane) and distinctive bacterial cell wall features.

Phylogeny and Classification of *Filos agilis* and *Nanos amicus*

Filos agilis gen. et sp. nov. and *Nanos amicus* gen. et sp. nov. are similar in morphology to *Siluania monomastiga*. All three flagellates are extremely tiny (2–3 μm) and possess a single mastigoneme-bearing flagellum that is about the same length as the cell (Figs 9A, 10B). In addition, all three of these genera are planktonic in freshwater habitats and display similar ultrastructural traits: a single nucleus, a single mitochondrion, and a cytostome/cytopharynx apparatus. TEM figures from Karpov et al. (1998) show that *Siluania* cell surfaces are covered with a fuzzy layer, like those observed here in *F. agilis* and *N. amicus*. A rapid, mostly straight swimming pattern is another commonality. However, while *Siluania* is only known to be planktonic, both *F. agilis* and *N. amicus* inhabit the mucilage of *A. lindahlii*.

Although *Filos*, *Nanos*, and *Siluania* share many morphological features, SSU rDNA gene sequence differences among these flagellates are over 8% (Table 1), providing a rationale for describing them as three separate genera. These genetic differences are greater than those between some morphologically and ecologically distinct species of Chrysophyceae+Synurophyceae. For example *A. lindahlii* differs from the photoautotrophic synurophycean *Mallomonas annulata* by 5.13% of SSU rDNA positions. In addition, *Siluania* is phylogenetically more closely related to morphologically distinct bicosoecid *Adriamonas* than to *Filos* or to *Nanos* (Fig. 13). Furthermore, *Filos* and *Nanos* are each closely related to uncultivated bicosoecid species in the SSU rDNA tree, supporting that these two flagellates are not sister taxa (Fig. 13). *Adriamonas*, a soil dwelling biflagellate that lacks mastigonemes on the flagella, is closely related to *Siluania*, but is more than four times larger than *Siluania* and contains multiple mitochondria (Verhagen et al. 1994). *Paramonas* has one flagellum and rotates while swimming (Cavalier-Smith and Chao 2006), as do *Siluania*, *Filos* and *Nanos*, but is longer (4–11 μm long) than these flagellates. While ultrastructural data are not available for *Paramonas* and the closely related biflagellate *Nerada*, our ultrastructural and molecular phylogenetic findings for

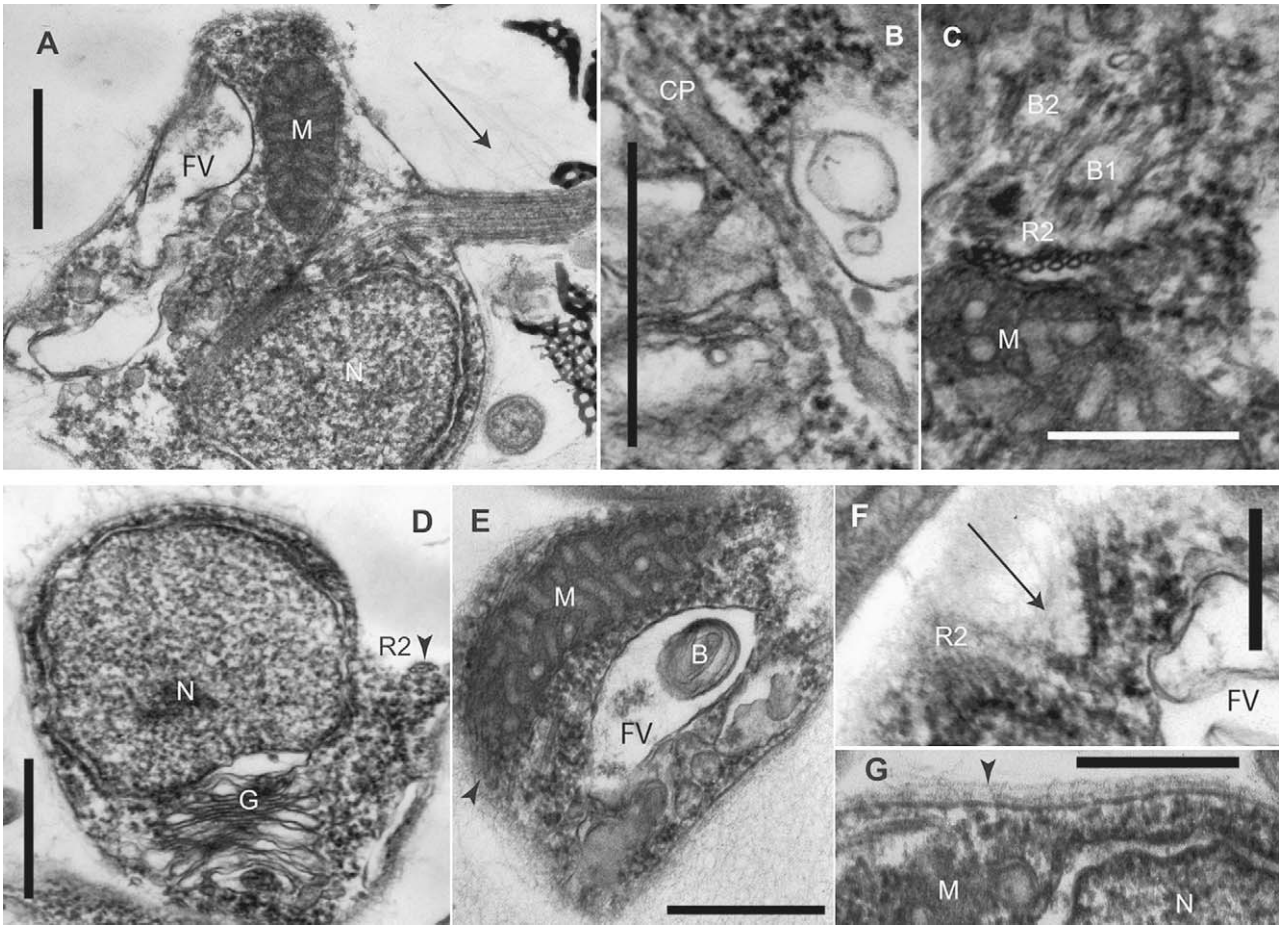

Figure 9. *Filos agilis*, transmission electron micrographs. – **A** A longitudinal section showing the single flagellum with fibrillar mastigonemes (arrow), the nucleus (N), the single mitochondrion with tubular cristae (M), and a food vacuole (FV). **B** A cytopharynx (CP). **C** An oblique section through two basal bodies (B1, B2). A broad rootlet (R2) composed of 8 microtubules lies between basal bodies and the mitochondrion (M). **D** A Golgi body (G) near the nucleus (N). **E** Degraded bacterial cell (B) in the food vacuole (FV). R2 rootlet (arrowhead) running across the mitochondrion. **F** A cytostome (arrow). **G** An organic layer covering the cell body (arrowhead). Scale bar=0.5 μm (A, B, D, E), 0.3 μm (C, F, G).

Filos and *Nanos* suggest that these flagellates may also possess a cytostome/cytopharynx apparatus.

In both *F. agilis* and *N. amicus*, a broad root, identified as root 2 (R2, formerly known as R3) according to bicosoecid flagellar nomenclature (Karpov et al. 2001), is composed of at least 8 and 6 microtubules, respectively (Figs 9C, 10D). R2 in Bicosoecida supports the feeding structure, known as the cytostome or lip (Karpov et al. 2001). A four-microtubular root observed in *N. amicus* probably corresponds to a portion of a split R2 (not shown), as described in other bicosoecids (O'Kelly and Patterson 1996). *Siluania monomastiga* has a smaller R2 arranged as 3+1 microtubules (Karpov et al. 2001), distinguishing this species from *F. agilis* or *N. amicus*. The two additional rootlets of 1 and 2 microtubules observed in *F. agilis* and *N. amicus* may correspond to R4 and R1, respectively.

Karpov et al. (1998) and Verhagen et al. (1994) suggested that scale-covered pseudodendromonads, such as *Cyathobodo* and *Pseudodendromonas*, might be closely related to *Adriamonas* or to *Siluania* based on ultrastructural features such as the presence of a well-developed cytostome/cytopharynx apparatus and other cytoskeletal structures. The presence of an organic layer in *F. agilis*, *N. amicus*, and *S. monomastiga*, if homologous to pseudodendromonad scales, would further strengthen this hypothesis. SSU rDNA

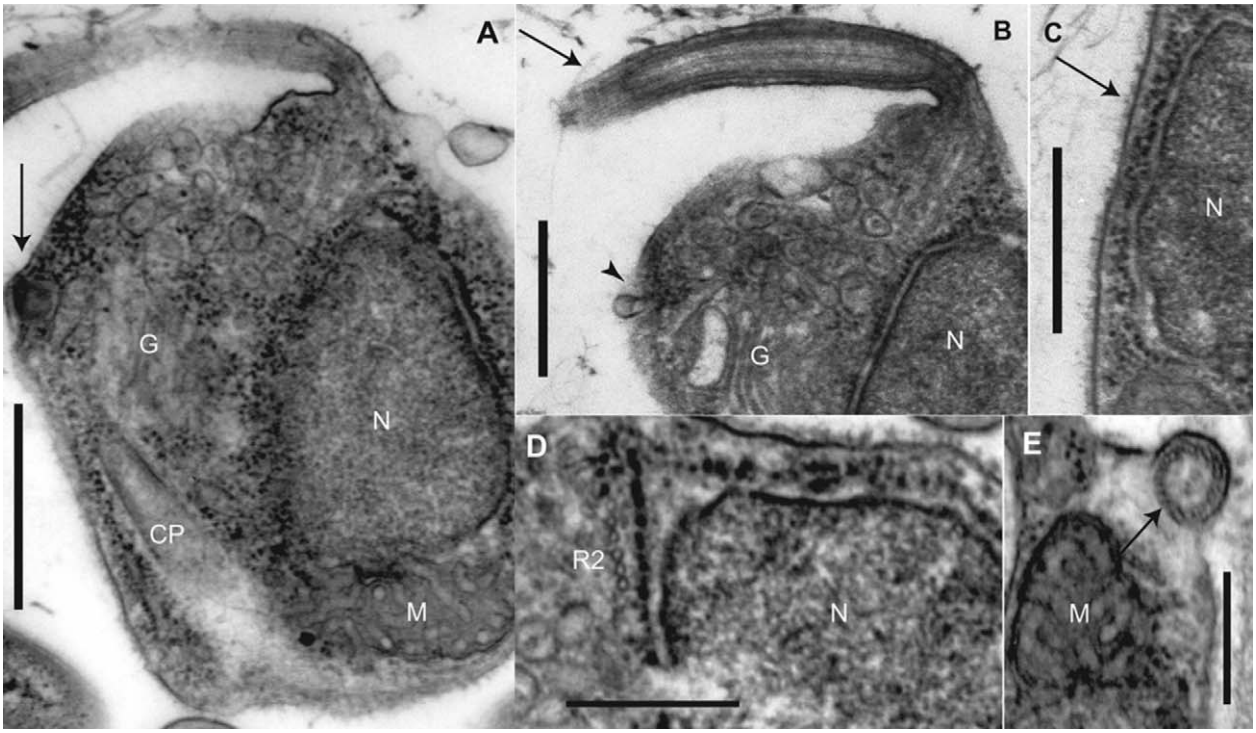

Figure 10. *Nanos amicus*, transmission electron micrographs. – **A** A longitudinal section showing the flagellum, a single nucleus (N), a Golgi body (G), a single mitochondrion with tubular cristae (M), cytostome (arrow) and cytopharynx (CP). **B** Mastigonemes on the flagellum (arrow) and a cytostome (arrowhead). A Golgi body (G) occurs between the cytostome and the nucleus (N). **C** An organic layer on cell surface (arrow). **D** The R2 rootlet composed of 6 microtubules extends down the nuclear surface. **E** A cross section of the basal body (arrow). Mitochondrion (M). Scale bar=0.5 μm (A, B, C), 0.3 μm (D, E).

sequence data from members of pseudodendromonads are needed to test this hypothesis.

F. agilis or *N. amicus* as Epibionts of *A. lindahlii*

Several separate cultures of *A. lindahlii* were established from at least three different lake samples with the use of the single-colony isolation technique. We observed that all of the *A. lindahlii* cultures were "contaminated" with similar kinds of picoflagellates that were embedded in the colonial matrix. We subsequently identified two of these, isolated from two separate lakes, as *F. agilis* and *N. amicus*. Such associations are unlikely to have resulted from accidental co-isolation of smaller flagellates from enriched field samples, because none of our other protist cultures from the same acidic freshwater sites contained the same types of picoflagellates. These observations suggest that *F. agilis* and *N. amicus* are closely associated with *A. lindahlii* in their natural habitats.

The fact that we were able to later establish four separate uniprotistan cultures—two of *A. lindahlii* and separate cultures of *F. agilis* and *N. amicus*—suggests that the associations are not obligate. However, long-term observation of these cultures suggests that the picoflagellates may benefit by associating with *A. lindahlii*. While the maximum number of *A. lindahlii* cells did not seem to change whether or not picoflagellate epibionts were present, *F. agilis* or *N. amicus* were more abundant when grown with *A. lindahlii*. In the association with *A. lindahlii*, *F. agilis* and *N. amicus* may feed on the colonial mucilage secreted by *A. lindahlii* and the bacterial cells embedded in it. It is also possible that the *A. lindahlii* mucilage may collect organic materials from the water column, thereby concentrating them. If so, *F. agilis* and *N. amicus* may be able to save considerable energy in food capture by being embedded in the mucilage, perhaps explaining why these picoflagellates seem to grow faster in the association with *A. lindahlii* than separate from it.

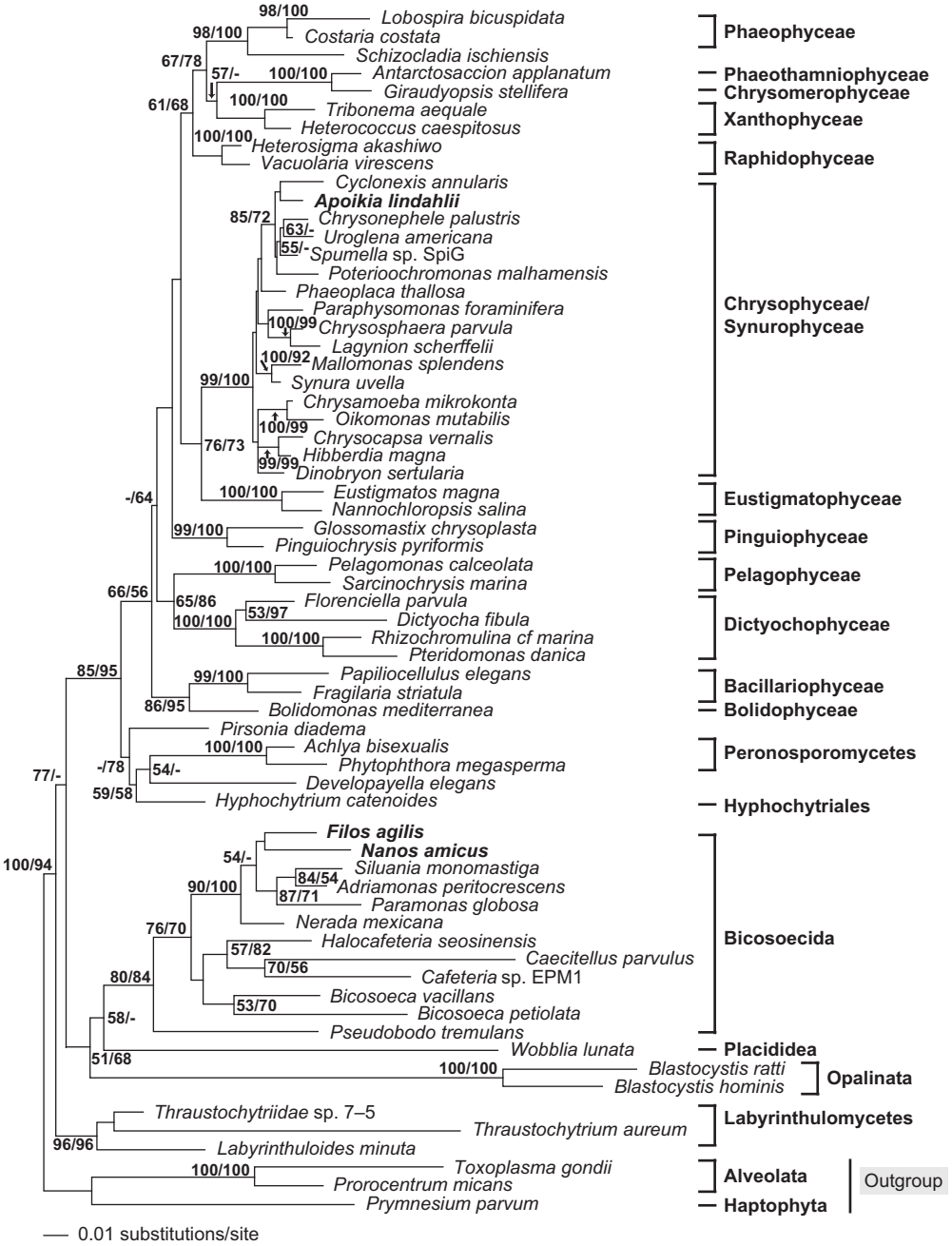

Figure 11. ML tree (GTR+Γ+I, 4 rate categories) based on SSU rDNA gene sequences of major subclades of stramenopiles. The data set included 65 taxa and 1490 unambiguously aligned sites. Lineages of alveolates and haptophytes were used as paraphyletic outgroups. ML and ME (minimum evoution) distance bootstrap values $\geq$50% are indicated at the corresponding nodes. Dashes represent bootstrap values $<$50%. New sequences obtained in this study are in bold.

Taxonomic Summary and Descriptions

Apoikia gen. nov. (ICBN)

Chrysophyta aphotosynthetica, crescens in coloniis, cellulis incoloratis in muco incolorato. Cellulae sphaericae vel ellipsoideae, instructae flagellis binis longitudine inaequalibus, absque coniunctionibus inter cellulas, caulibus mucosis, et squamis (Figs 1A, 2, 3A).

Species typical: *Apoikia lindahlii* (Skuja).

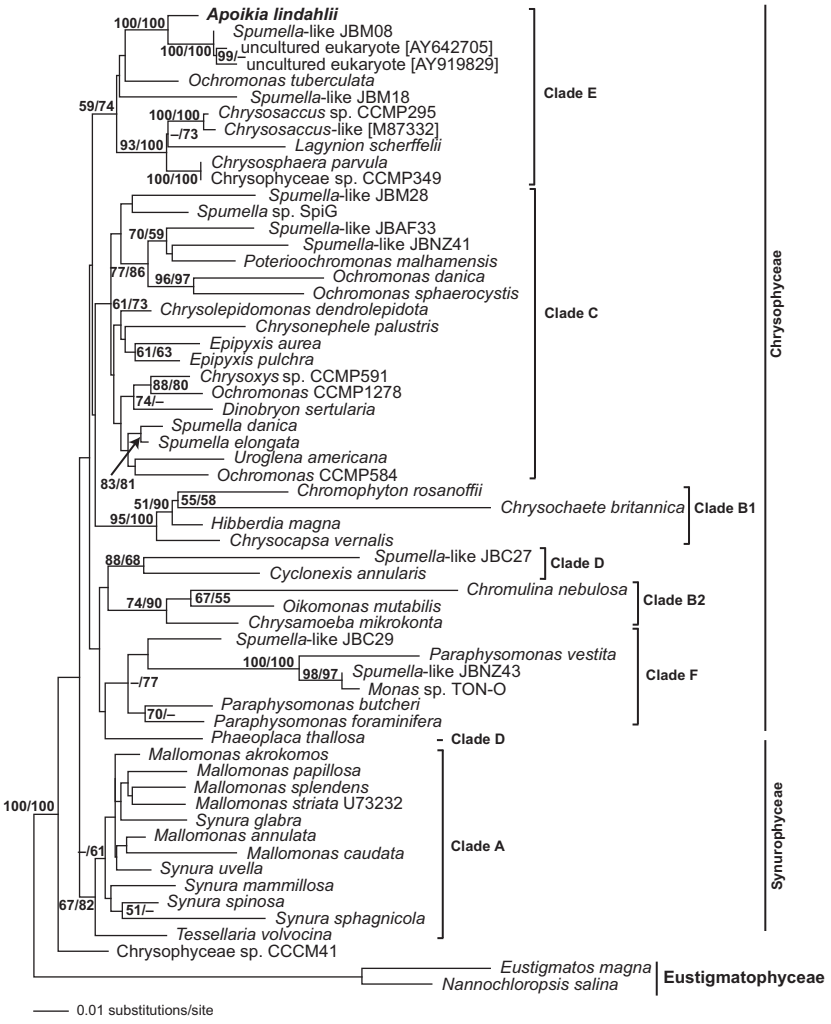

Figure 12. ME distance tree based on analysis of the Chrysophyceae and Synurophyceae taxa (GTR+Γ+I, 4 rate categories). The data set included 60 taxa and 1674 unambiguously aligned sites. Major subclades labeled Clade A–F of the Chrysophyceae+Synurales clade were proposed by Andersen et al. (1999). ME distance and ML (GTRCAT) bootstrap values $\geq$50% are indicated at the corresponding nodes.

Non-photosynthetic chrysophyte, growing in colonies, with colorless cells embedded in colorless mucilage. Cells spherical or ellipsoidal, provided with two flagella of unequal length, lacking intercellular connections, mucilage stalk, and scales.

Type species: *Apoikia lindahlii* (Skuja).

Apoikia lindahlii (Skuja) comb. nov. (ICBN)

Basionym. *Monas lindahliii* Skuja. Nova Acta Regiae Societatis Scientiarum Upsaliensis, Series IV 16(3): 319, 1956.

Etymology: *Apoikia* means colony.

Authentic culture: UW-Madison Culture Collection UWMO2004-3.

Distribution and habitat: Known from *Sphagnum*-dominated peat bogs.

Note: TEM block of *A. lindahlii* labeled v0230221WIS, WIS was deposited in the Wisconsin State Herbarium at the University of Wisconsin, Madison, WI, U.S.A. The culture was collected at Jyme Lake, Oneida County, Wisconsin, U.S.A. (45.8395, -89.6634). 18S rDNA sequence was deposited in GenBank under the accession numbers FJ971854-FJ971855.

Filos gen. nov (ICBN)

Bicosoecid absque lorica, vivens intra *Apoikiae* mucum. Cellulae 2.5 μm longae. Cellula quaeque instructa flagello singulari emergi et structura

consumenti cytostomate/cytopharynge; superficies cellularum strato carbonaceo tecta. Mitochondrion singulare prope corpora basalia locatum. Radicella duae ex microtubulis octo constans. Seiunctio ex *Apoikiae lindahliie* muco. 18S rDNA series propria: GenBank accession number FJ971856.

Species typical: *Filos agilis*

Bicosoecid lacking a lorica, living within the mucilage of *Apoikia*. Cells 2.5 μm long. Cell with a single emergent flagellum, cytostome/cytopharynx ingestion apparatus, and cell surface covered with an organic layer. A single mitochondrion located close to the basal bodies. Rootlet 2 comprising 8 microtubules. Isolated from *Apoikia lindahlii* mucilage. Distinctive 18S rDNA sequence: GenBank accession number FJ971856.

Type species: *Filos agilis*

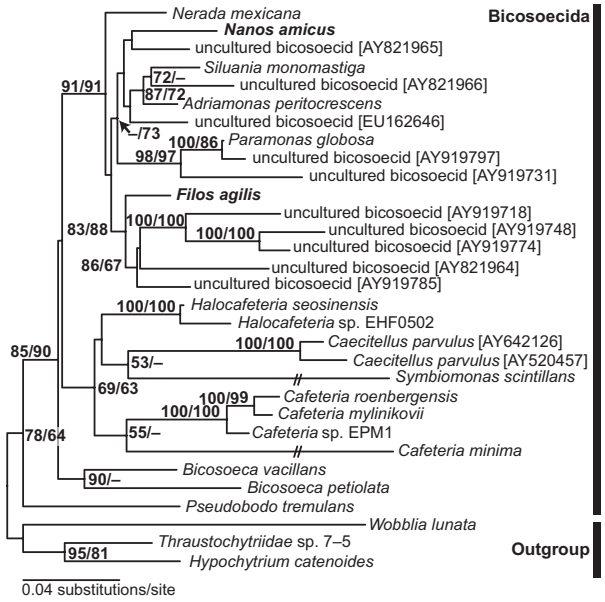

Figure 13. ME distance tree based on analyses of bicosoecid taxa (GTR+Γ+I, 4 rate categories). The data included 1560 nucleotides. ME distance and ML (GTRCAT) bootstrap values ≥50% are indicated at the corresponding nodes. Exclusion of the divergent SSU rDNA sequences of *Symbiomonas scintillans* and *Cafeteria minima* did not change the tree topology although bootstrap values were increased for some nodes (data not shown).

Filos agilis sp. nov. (ICBN)

With the characters of the genus.

Holotype: TEM block labeled v0230222WIS, WIS deposited in the Wisconsin State Herbarium at the University of Wisconsin, Madison, WI, U.S.A.

Isotype: Fig. 9A.

Type locality: Hook Lake, Dane Co., Wisconsin, U.S.A. (42.9535, -89.3383)

Etymology: *Filos* (m.), friend, alludes to its epibiontic relationship with *Apoikia*; *agilis*, agile, refers to its swimming motion.

Type culture: UW-Madison Culture Collection UWMO2004-5.

Distribution and habitat: Known from Hook Lake, Dane Co., WI, an acidic freshwater bog lake, occurring within the mucilage of *Apoikia lindahlii* (can be cultured separately).

Nanos gen. nov. (ICBN)

Bicosoecid absque lorica, vivens intra *Apoikiae* mucum. Cellulae 2.8 μm longae. Cellula quaeque instructa flagello singulari emergi et structura consumenti cytostomate/cytopharynge; superficies cellularum strato carbonaceo tecta. Mitochondrion singulare in extremo postico locatum. Radicella duae ex microtubulis sex constans. Seiunctio ex *Apoikiae lindahliie* muco. 18S rDNA series propria: GenBank accession number FJ971853.

Species typical: *Nanos amicus*

Bicosoecid lacking a lorica, living within the mucilage of *Apoikia*. Cells 2.8 μm long. Cell with a single emergent flagellum, cytostome/cytopharynx ingestion apparatus, and cell surface covered with organic layer. A single mitochondria located in the posterior end. Rootlet 2 comprising 6 microtubules. Isolated from *A. lindahlii* mucilage.

Table 1. SSU rDNA gene sequence comparison among three morphologically similar bicosoecids. The BLASTN with the default setting was used to calculate the number of different nucleotide positions and the percentage of gaps in each alignment.

	Percent of differing sites (excluding gaps)	Gaps
Filos agilis & *Nanos amicus*	149/1744 (8.54%)	65/1744 (3.73%)
N. amicus & *Siluania monomastiga*	207/1772 (11.68%)	97/1772 (5.47%)
S. monomastiga & *F. agilis*	175/1762 (9.93%)	90/1762 (5.11%)

Distinctive 18S rDNA sequence: GenBank accession number FJ971853.

Type species: *Nanos amicus*

Nanos amicus sp. nov. (ICBN)

With the characters of the genus.

Holotype: TEM block labeled v0230223WIS, WIS deposited in the Wisconsin State Herbarium at the University of Wisconsin, Madison, WI, U.S.A.

Isotype: Fig. 10A.

Type locality: Jyme Lake, Oneida County, Wisconsin, U.S.A. (45.8395, -89.6634)

Etymology: *Nanos* (m.) refers to its tiny size; *amicus*, friend, refers to its epibiontic association with *Apoikia*.

Type culture: UW-Madison Culture Collection UWMO2004-3.

Distribution and habitat: Known from Jyme Lake, Oneida Co., WI, an acidic freshwater bog lake, occurring within the mucilage of *Apoikia lindahlii* (can be cultured separately).

Methods

Isolation and culturing: Samples were collected during the summer from two *Sphagnum*-dominated acidic freshwater bodies: Jyme Lake (Oneida County, WI, 45.8395, -89.6634) and Hook Lake (Dane County, WI, 42.9535, -89.3383). Both Jyme Lake and Hook Lake are peat bogs with open water area surrounded by a floating mat of *Sphagnum* mosses and other shrubs. At the time of sampling, the pH was around 5 for both sites. Jyme Lake was the focus of a previous analysis of the relationship of pH, DOC, and bacterial activities in different microsites (Fisher et al. 1998). Hook Lake was previously the site of a study of bacterial epibionts of photosynthetic protists (Fisher and Wilcox 1996). Large metazoan grazers were removed by use of an ~25 μm Whatman filter and subsamples were enriched with soil extract and incubated for 3–5 days in the dark. Individual colonies of *Apoikia lindahlii* were isolated with a finely-drawn glass pipette (Stein 1973) and cultured in a 20:1 mixture of filtered, sterilized lake water and soil extract. When cultures were established, we noticed smaller flagellates inhabiting the mucilaginous matrix produced by the colonial flagellate *A. lindahlii*. Individual cells were re-isolated and four distinct clonal uniprotistan cultures were established for molecular sequencing. Cultures were maintained in a culture room at 15 °C. Cultures of *A. lindahlii* were exposed to light for periods of 7–20 days to check for photosynthetic pigment formation. Cultures—*Filos agilis* and *Nanos amicus* in co-culture with *Apoikia lindahlii*—are available upon request from UW-Madison Culture Collection (contact info: lkgraham @wisc.edu).

DNA preparation, PCR amplification, cloning, and sequencing: Cells were collected in an Eppendorf tube by centrifuging for 5 min at the maximum speed, and the supernatant was carefully removed by pipetting. Genomic DNA was purified using the DNeasy Plant Mini Kit (Qiagen, Valencia, CA, Catalog no. 69104), according to the manufacturer's suggested protocols.

Two-step nested PCR was used to amplify sufficient DNA for subsequent cloning reactions. The SSU rDNA gene was amplified using the following two primer pairs: the outer pairs 5′-CTG GTT GAT CCT GCC AGT AGT-3′ (nu-SSU-0024-5′) and 5′-TGA TCC TTC YGC AGG TTC ACC-3′ (nu-SSU-1768-3′); and the inner pairs 5′-CCT GCC AGT AGT CAT AYG CTT-3′ (nu-SSU-0033-5′) and 5′-CAG GTT CAC CTA CGG AAA CCT-3′ (nu-SSU-1757-53). The standard 50 μl reaction mixture consisted of 2.5 units of Takara Ex Taq (Takara, Tokyo, code no. RR001A), 1X Ex Taq buffer, 0.2 mM of each dNTP, 0.6 μM of each primer, and 5% glycerol. The PCR cyclic reactions consisted of a denaturation step of 3 min at 95 °C; 30 cycles of 1 min at 95 °C, 1 min at 45 °C, and 2 min at 72 °C; and a final 15 min cycle at 72 °C. PCR-amplified fragments were either gel-purified or cleaned using Wizard® SV Gel and PCR Clean-Up System (Promega, Madison, WI, catalog no. A9281). The cleaned amplified fragments were cloned into pGEM®-T Easy vector (Promega, Madison, WI, catalog no. A1380). Multiple bacterial clones were obtained from each cloning reaction. Plasmids were isolated from multiple positive bacterial clones using the QIAquick Miniprep Kit (Qiagen, Valencia, CA, catalog no. 27104). Sequencing reactions were performed with 20 μl of reaction mixture, which included 2 μl of BigDye Terminator v. 3.1 mix (Applied Biosysems), 3 μl of dilution buffer (Applied Biosystems), 0.6 μM sequencing primer, and 100–200 ng of template DNA. Cyclic sequencing reactions were an initial denaturation of 3 min at 95 °C, then 50 cycles of 10 sec at 96 °C, 4 min at 58 °C, and 7 min at 72 °C. Excess dye terminators were removed using Agencourt CleanSEQ 96 Starter Kit (Agencourt Biosciences, Beverly, MA, product no. 000145). Sequences were determined at the University of Wisconsin Biotechnology Center and have been deposited in GenBank (accession numbers FJ971853–FJ971856).

Sequence alignments and phylogenetic analysis: MacClade (ver. 4.05; Maddison and Maddison 2001) was used to manually align sequences obtained in this study and other sequences downloaded from GenBank. Ambiguous positions were deleted. PAUP* (ver. 4.0b; Swofford 2002) and RAxML (ver. 7.0.4; Stamatakis 2006) were utilized for the maximum likelihood (ML) and distance analyses of SSU rDNA gene sequences. Modeltest (ver. 3.7; Posada and Crandall 1998) was used to find the best fit model of nucleotide evolution and to estimate substitution rates, base frequencies, Γ distribution parameter (α), and proportion of invariable sites. For ML and minimum evolution distance tree search using PAUP*, the input order of sequences was randomized and the process was repeated 100 times with the tree bisection and reconnection branch-swapping algorithm. For RAxML analysis, ML trees were inferred with the GTRCAT model from 100 distinct randomized maximum parsimony starting trees. Bootstrap values were obtained from 100 re-samplings.

Light and electron microscopy: For scanning electron microscopy (SEM) of *A. lindahlii*, the culture was mixed with fixative containing 5% glutaraldehyde, 0.2 M sucrose in 0.2 M sodium cacodylate buffer (pH 7.2) and was mounted on cover slip coated by poly-L-lysine at room temperature for 30 min. The sample was rinsed with the 0.2 M buffer three times. The specimen was then fixed with 1% (w/v) osmium tetroxide in 0.2 M the buffer at room temperature for 30 min followed by dehydration through an ethanol series. Samples were critical point dried with CO_2 using a Tousimis Critical Point Dryer. Samples were then coated with gold using Cressington 208HR high Resolution Sputter Coater, and observed with a Hitachi S-4700 field-emission scanning electron microscope.

For transmission electron microscopy (TEM) of *A. lindahlii,* the culture was mixed with fixative containing 5% glutaraldehyde and 0.2 M sucrose in 0.2 M sodium cacodylate buffer (pH 7.2) at room temperature for 1 h. Cells were aggregated into a pellet by centrifugation at 1000 g for 5 min and rinsed with the 0.2 M buffer three times. The specimen was then fixed with 1% (w/v) osmium tetroxide in 0.2 M buffer at room temperature for 30 min followed by dehydration through an ethanol series (1 h at 30%, 30 min at 50%, 15 min each at 70%, 85%, 90%, 95%, and 100 %) and substitution with acetone with 1:1 absolute acetone: ethanol and then 100% acetone twice, followed by three changes of freshly-prepared resin (Epon 812). Resin was polymerized for 14 hours at 65 °C. Ultra thin sections (50 nm) were collected onto copper grids, stained with uranyl acetate and lead citrate, and examined and photographed with Hitachi H-7600.

For TEM of *F. agilis* and *N. amicus,* cell cultures were mixed with an equal volume of buffered glutaraldehyde. The final concentration was 1% glutaraldehyde in 0.025 M cacodylate buffer (pH 5.3). The primary fixation lasted at least one hour at room temperature. Because cells were very fragile, we designed a concentration apparatus to gently collect cells on 0.8 μm MF-Millipore membrane filter (Millipore Corporation, Billerica, MA, catalog no. AAWP01300). The cell concentration apparatus consisted of the lower part of a Millipore Swinnex syringe filter holder with screen (13 mm) (Millipore corporation, Billerica, MA, catalog no. SX00-013-00) connected to a vacuum-filtering flask by use of a pipette tip and a rubber tube. A hand pump was used to gently filter culture fluid that was dripped onto filters by means of a pipette. Care was taken to prevent flagellate cells from drying during filtration. Heterotrophic cells were deposited onto a base layer of green *Mesostigma* cells. These green cells turned black during later treatment with osmium tetroxide, thereby serving as a visual marker for locating small paler heterotrophs within plastic after embedding. After approximately 50-100 ml of cell culture were filtered, the cells were immediately encased in 1% low-melting agarose gel. Agarose pieces were washed twice in cacodylate buffer for 10 min and the membrane filters were peeled off using forceps. Post-fixation was conducted with 1% osmium tetroxide in distilled water for one hour, followed by *en bloc* staining with 0.1% aqueous uranyl acetate at 4 °C overnight, and dehydration in an ethanol concentration series (10 min each at 15%, 30%, 50%, 70%, 80%, 85%, 90%, 95%, and three changes of absolute ethanol for 20 min). Agarose pieces were infiltrated with 1:1 and then 1:3 absolute ethanol: Spurr's resin mixture (Electron Microscopy Sciences, Hatfield, PA, catalog no. 14300), followed by three changes of freshly-prepared Spurr's resin of 5-18 hrs each, in a desiccator under vacuum. Resin was polymerized for 18 hours at 60 °C. Ultra thin sections were collected onto copper grids, stained with lead citrate, and examined and photographed with Hitachi H-7000 and Zeiss EM10C electron microscopes.

Light microscopic observations of fresh and glutaraldehyde fixed cells were made with a Nikon phase-contrast microscope and photographs were taken with an Olympus digital camera at 1,000X. Figure 1H was taken using a Zeiss Axioplan 2 imaging microscope connected to a Leica DC500 digital chilled CCD camera. To check for a basal swelling in the posterior flagellum of *A. lindahlii*, living cells were observed under a Zeiss Axioplan HBO (50W mercury) fluorescence microscope using a 395-440 FT460LP470 violet filter (#48 77 05) and an excitation wavelength of 395–440 nm. *Synura sphagnicola* was used as a positive control for the presence of a green fluorescent flagellar basal swelling.

Acknowledgements

This research was supported by grant MCB-9977903 from the National Science Foundation and an Anna Grant Birge Memorial Award (University of Wisconsin-Madison). This work was also supported by grants to BSL from the Tula Foundation (Centre for Microbial Diversity and Evolution), the National Science and Engineering Research Council of Canada (NSERC 283091-09) and the Canadian Institute for Advanced Research, Program in Integrated Microbial Biodiversity. The authors also thank J. Graham (University of Wisconsin-Madison) for help with the TEM preparation of *Filos* and *Nanos*; L. Wilcox (University of Wisconsin-Madison) for helpful discussions; C. Sattler (University of Wisconsin-Madison), R. Wise and T. Kostman (University of Wisconsin-Oshkosh) for technical advice; K. Elliot (University of Wisconsin-Madison) for help with illustrations; R. Kowal (University of Wisconsin-Madison) for edition of Latin descriptions; and the University of Chicago for access to print journals in the John Crerar Library.

References

Andersen RA (1987) The Synurophyceae classis nov., a new class of algae. Am J Bot **74**:337–353

Andersen RA (1989) Absolute orientation of the flagellar apparatus of *Hibberdia magna* comb. nov. (Chrysophyeae). Nord J Bot **8**:653–669

Andersen RA (1990) The three-dimensional structure of the flagellar apparatus of *Chrysosphaerella brevispina* (Chrysophyceae) as viewed by high voltage electron microscopy stereo pairs. Phycologia **29**:86–97

Andersen RA (2004) Biology and systematics of heterokont and haptophyte algae. Am J Bot **91**:1508–1522

Andersen RA, Wetherbee R (1992) Microtubules of the flagellar apparatus are active during prey capture in the chrysophycean alga *Epipyxis pulchra*. Protoplasma **166**:8–20

Andersen RA, Van de Peer Y, Potter D, Sexton JP, Kawachi M, LaJeunesse T (1999) Phylogenetic analysis of the SSU RNA from members of Chrysophyceae. Protist **150**:71–84

Belcher JH, Swale EMF (1972) The morphology and fine structure of the colorless colonial flagellate *Anthophysa vegetans* (o. f. Müller) Stein. Br Phycol J **7**:335–346

Berney C, Fahrni J, Pawlowski J (2004) How many novel eukaryotic 'kingdoms'? Pitfalls and limitations of environmental DNA surveys. BMC Biol **2**:13

Boenigk J (2008) The past and present classification problem with nanoflagellates exemplified by the genus *Monas*. Protist **159**:319–337

Boenigk J, Pfandl K, Stadler P, Chatzinotas A (2005) High diversity of the '*Spumella*-like' flagellates: an investigation based on the SSU rRNA gene sequences of isolates from habitats located in six different geographic regions. Environ Microbiol **7**:685–697

Cavalier-Smith T, Chao EE (2006) Phylogeny and megasystematics of phagotrophic heterokonts (Kingdom Chromista). J Mol Evol **62**:388–420

Crum H (1992) In: A Focus on Peatlands and Peat Mosses. The University of Michigan Press, Ann Arbor, Michigan

Fisher MM, Wilcox LE (1996) Desmid–bacterial associations in *Sphagnum*-dominated Wisconsin peatlands. J Phycol **32**:543–549

Fisher MM, Graham JM, Graham LE (1998) Bacterial abundance and activity across sites within two Northern Wisconsin *Sphagnum* bogs. Microb Ecol **36**:259–269

Gibbs SP (1979) The route of entry of cytoplasmically synthesized proteins into chloroplasts of algae possessing chloroplast ER. J Cell Sci **35**:253–266

Gorham E (1991) Northern peatlands: role in the carbon cycle and probable responses to climatic warning. Ecol Appl **1**:182–195

Graham JM, Kent AD, Lauster GH, Yannarell AC, Graham LE, Triplett EW (2004) Seasonal dynamics of phytoplankton and planktonic protozoan communities in a northern temperate humic lake: diversity in a dinoflagellate dominated system. Microb Ecol **48**:528–540

Hibberd DJ (1979) The structure and phylgenetic significance of the flagellar transition region in the chlorophyll *c*-containing algae. BioSystems **11**:243–261

Ikävalko J, Kristiansen J, Thomsen HB (1994) A revision of the taxonomic position of *Syncrypta glomerifera* (Chrysophyceae), establishment of a new genus *Lepidochrysis* and observations on the occurrence of *L. glomerifera* comb. nov. in brackish water. Nord J Bot **14**: 339–344

Jones RI (2000) Mixotrophy in planktonic protists: an overview. Freshwater Biol **45**:219–226

Karpov SA, Kersanach R, Williams DM (1998) Ultrastructure and 18S rRNA gene sequence of a small heterotrophic flagellate *Siluania monomastiga* gen. et sp. nov. (Bicosoecida). Eur J Protistol **34**:415–425

Karpov SA, Sogin ML, Silberman JD (2001) Rootlet homology, taxonomy, and phylogeny of bicosoecids based on 18S rRNA gene sequences. Protistology **2**:34–47

Kristiansen J, Preisig HR, eds (2001) Encyclopedia of Chrysophyte Genera. Bibliotheca Phycologica, Vol. 110 J. Cramer, Berlin, Stuttgart

López-García P, Rodríguez-Valera F, Pedrós-Alió C, Moreira D (2001) Unexpected diversity of small eukaryotes in deep-sea Antarctic plankton. Nature **409**:603–607

Maddison DR, Maddison WP (2001) MacClade 4: Analysis of Phylogeny and Character Evolution. Version 4.03. Sinauer Associates, Sunderland, Massachusetts

Massana R, Terrado R, Forn I, Lovejoy C, Pedrós-Alió C (2006) Distribution and abundance of uncultured heterotrophic flagellates in the world oceans. Environ Microbiol **8**: 1515–1522

Moestrup Ø (2000) The Flagellate Cytoskeleton: Introduction of a General Terminology for Microtubular Flagellar Roots in Protists. In Leadbeater SC, Green JC (eds) The Flagellates: Unity, Diversity and Evolution. Taylor and Francis, London, pp 69–94

Moriya M, Nakayama T, Inouye I (2000) Ultrastructure and 18S rDNA sequence analysis of *Wobblia lunata* gen et sp. nov., a new heterotrophic flagellate (stramenopiles, incertae sedis). Protist **151**:41–55

Müller OF (1773) Vermium Terrestrium et Fluviatilium, vol. 1(1). Havniae et Lipsiae, Copenhagen.

O'Kelly CJ, Patterson DJ (1996) The flagellar apparatus of *Cafeteria roenbergensis* Fenchel & Patterson, 1988 (Bicosoecales=Bicosoecida). Eur J Protistol **32**:216–226

Posada D, Crandall KA (1998) Modeltest: testing the model of DNA substitution. Bioinformatics **14**:817–818

Preisig HR, Hibberd DJ (1983) Ultrastructure and taxonomy of *Paraphysomonas* (Chrysophyceae) and related genera 3. Nord J Bot **3**:695–723

Preisig HR, Hibberd DJ (1984) Virus-like particles and endophytic bacteria in *Paraphysomonas* and *Chromophysomonas* (Chrysophyceae). Nord J Bot **4**: 279–285

Preisig HR, Vørs N, Hällfors G (1991) Diversity of Heterotrophic Heterokonts. In Patterson DJ, Larsen J (eds) The Biology of Free-living Heterotrophic Flagellates. Clarendon Press, Oxford, pp 361–399

Pringsheim EG (1946) On iron flagellates. Philos Trans R Soc London Ser B Biol Sci **232**:311–342

Schnepf E, Deichgräber G, Röderer G, Herth W (1977) The flagellar root apparatus, the microtubular system and associated organelles in the chrysophycean flagellate, *Poterioochromonas malhamensis* Peterfi (syn. *Poteriochromonas stipitata* Scherffel and *Ochromonas malhamensis* Pringsheim). Protoplasma **92**:87–107

Sekiguchi H, Moriya M, Nakayama T, Inouye I (2002) Vestigial chloroplasts in heterotrophic stramenopiles *Pteridomonas danica* and *Ciliophrys infusionum* (Dictyochophyceae). Protist **153**:157–167

Silva PC (1960) Remarks on algal nomenclature III. Taxon **9**:18–25

Skuja H (1956) Taxonomische und biologische Studien über das Phytoplankton schwedischer Binnengewässer. Nova Acta Regiae Soc Sci Ups Ser IV **16**:1–404

Stamatakis A (2006) RAxML-VI-HPC: maximum likelihood-based phylogenetic analyses with thousands of taxa and mixed models. Bioinformatics **22**:2688–2690

Stoeck T, Jost S, Boenigk J (2008) Multigene phylogenies of clonal *Spumella*-like strains, a cryptic heterotrophic nanoflagellate, isolated from different geographical regions. Int J Syst Evol Microbiol **58**:716–724

Stein JR ed (1973) Handbook of Phycological Methods: Culture Methods and Growth Measurements. Cambridge University Press, Cambridge

Swofford DL (2002) In: PAUP*: Phylogenetic Analysis Using Parsimony (*and other methods). Version 4. Sinauer Associates, Sunderland, Massachusetts

Verhagen FJM, Zölffel M, Brugerolle G, Patterson DJ (1994) *Adriamonas peritocrescens* gen. nov., sp. nov., a new free-living soil flagellate (Protista, Pseudodendromonadidae Incertae Sedis). Eur J Protistol **30**:295–308

Wetherbee R, Andersen RA (1991) Flagella of a chrysophycean alga play an active role in prey capture and selection. Direct observation on *Epipyxis pulchra* using image enhanced video microscopy. Protoplasma **166**:1–7

Wujek DE (1984) Bacteria in the perinuclear cisternae of the chrysophyte *Chrysosphaerella*. Trans Kans Acad Sci **87**: 32–35

Yubuki N, Nakayama T, Inouye I (2008) A unique life cycle and perennation in a colorless chrysophyte *Spumella* sp. J Phycol **44**:164–172